

# PHYSICAL MODEL OF THE TROMBONE USING DYNAMIC GRIDS FOR FINITE DIFFERENCE SCHEMES

Silvin Willemsen

Multisensory Experience Lab  
Aalborg University Copenhagen  
Copenhagen, Denmark  
sil@create.aau.dk

Stefan Bilbao, Michele Ducceschi

Acoustics and Audio Group  
University of Edinburgh  
Edinburgh, UK

Stefania Serafin

Multisensory Experience Lab  
Aalborg University Copenhagen  
Copenhagen, Denmark

## ABSTRACT

The trombone...

## 1. INTRODUCTION

Introintro

Main challenge is to include time-varying length

## 2. CONTINUOUS

The behaviour of the air in an acoustic tube can be approximated using a 1-dimensional model.

Consider a tube of **time-varying** length  $L = L(t)$  (in m) defined over spatial domain  $x \in [0, L]$  and time  $t \geq 0$ . A system of first-order PDEs can then be written as

$$\frac{S}{\rho_0 c^2} \partial_t p = -\partial_x (Sv) \quad (1a)$$

$$\rho_0 \partial_t v = -\partial_x p \quad (1b)$$

with pressure  $p = p(x, t)$  (in N/m<sup>2</sup>), particle velocity  $v = v(x, t)$  (in m/s) and cross-sectional area  $S(x)$  (in m<sup>2</sup>). Furthermore,  $\rho_0$  is the density of air (in kg/m<sup>3</sup>) and  $c$  is the speed of sound in air (in m/s).

### 2.1. Coupling to a Lip Reed

To excite the system, a lip reed can be modelled as a simple oscillating mass according to

$$M_r \frac{d^2 y}{dt^2} = -Ky - M_r \sigma_r \frac{dy}{dt} + S_r \Delta p, \quad (2)$$

with displacement from the equilibrium  $y = y(t)$ , lip mass  $M_r$  (in kg), externally supplied (angular) frequency of oscillation  $w_0 = w_0(t) = \sqrt{K/M_r}$  (in rad/s), stiffness  $K = K(t)$  (in N/m), effective surface area  $S_r$  (in m<sup>2</sup>) and

$$\Delta p = P_m - p(0, t) \quad (3)$$

is the difference between the pressure in the mouth  $P_m$  and the pressure in the mouth piece  $p(0, t)$  (all in Pa). See Figure 2 for a

Copyright: © 2021 Silvin Willemsen et al. This is an open-access article distributed under the terms of the Creative Commons Attribution 3.0 Unported License, which permits unrestricted use, distribution, and reproduction in any medium, provided the original author and source are credited.

schematic of the lip reed model. This pressure difference causes a volume flow velocity following the Bernoulli equation

$$U_B = w_r [y + H_0]_+ \text{sgn}(\Delta p) \sqrt{\frac{2|\Delta p|}{\rho_0}}, \quad (4)$$

(in m/s) with effective lip-reed width  $w_r$  (m), static equilibrium separation  $H_0$  (in m) and  $[\cdot]_+ = 0.5(\cdot + |\cdot|)$  describes the “positive part of”. Notice that when  $y + H_0 \leq 0$ , the lips are closed and the volume velocity  $U_B$  is 0. Another volume flow is generated by the lip reed itself according to

$$U_r = S_r \frac{dy}{dt} \quad (5)$$

(in m/s). Assuming that the volume flow velocity is conserved the total air volume entering the system is defined as

$$S(0)v(0, t) = U_B(t) + U_r(t). \quad (6)$$

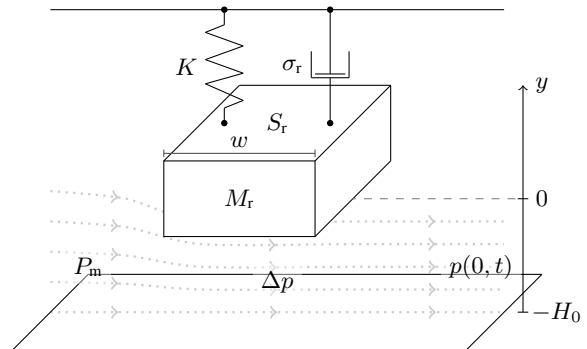


Figure 1: Lipsystem with the equilibrium at 0 and the distance from the lower lip  $H_0$ .

### 2.2. Radiation

The radiation model used is the one for the unflanged cylindrical pipe proposed by Levine and Schwinger in [1] and discretised by Silva et al. in [2]. As it is not important for the contribution of this work it will not be detailed here in full. The reader is instead referred to [3] for a comprehensive explanation.

### 3. DISCRETISATION

$l = [0, \dots, N]$  where

As done in [3], it is useful to place either  $p$  or  $v$  on an interleaved grid; both in space and time. Following Harrison, we place  $v$  on this interleaved grid. Accordingly, system (1) is discretised into the following finite difference scheme (FDS)

$$\frac{\bar{S}_l}{\rho_0 c^2} \delta_t p_l^n = -\delta_x (S_{l+1/2} v_{l+1/2}^{n+1/2}), \quad (7a)$$

$$\rho_0 \delta_t v_{l+1/2}^{n+1/2} = -\delta_x p_l^n, \quad (7b)$$

Boundary conditions:

At  $l = 0$

after which the update schemes become

$$p_l^{n+1} = p_l^n - \frac{\rho_0 c \lambda}{\bar{S}_l} (S_{l+1/2} v_{l+1/2}^{n+1/2} - S_{l-1/2} v_{l-1/2}^{n+1/2}), \quad (8a)$$

$$v_{l+1/2}^{n+1/2} = v_{l+1/2}^{n-1/2} - \frac{\lambda}{\rho_0 c} (p_{l+1}^n - p_l^n), \quad (8b)$$

where  $\lambda = ck/h$  is referred to as the Courant number and

$$\lambda \leq 1 \quad (9)$$

in order for the scheme to be stable.

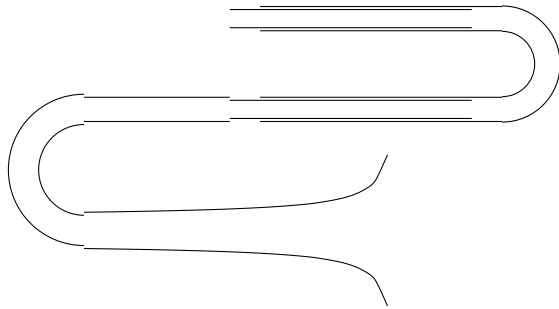


Figure 2: Lipsystem with the equilibrium at 0 and the distance from the lower lip  $H_0$ .

### 4. DYNAMIC GRID

We can split the FDS shown in (7) into two systems connected at their inner boundaries. The system is split at the end of the slide

For simplicity, the points are added at the far end of the slide so that there is an (approximately) equal slide-length on both sides of where the points are added.

$$\frac{\bar{S}_l}{\rho_0 c^2} \delta_t p_l^n = -\delta_x (S_{l+1/2} v_{l+1/2}^{n+1/2}), \quad (10a)$$

$$\rho_0 \delta_t v_{l+1/2}^{n+1/2} = -\delta_x p_l^n, \quad (10b)$$

$$\frac{\bar{S}_m}{\rho_0 c^2} \delta_t q_m^n = -\delta_x (S_{m+1/2} w_{m+1/2}^{n+1/2}), \quad (11a)$$

$$\rho_0 \delta_t w_{m+1/2}^{n+1/2} = -\delta_x q_l^n, \quad (11b)$$

Name	Symbol (unit)	Value
<b>Tube</b>		
Length	$L$ (m)	$2.685 \leq L \leq 3.718^*$
Air density	$\rho_0$ (kg/m <sup>3</sup> )	1.1769**
Wave speed	$c$ (m/s)	347.23**
Geometry	$S$ (m <sup>2</sup> )	See Table ??
<b>Lip reed</b>		
Mass	$M_r$ (kg)	$5.37 \cdot 10^{-5}^*$
Frequency	$\omega_0$ (rad/s)	$?? \leq \omega_0 \leq ??$
Mouth pressure	$P_m$ (Pa)	$0 \leq P_m \leq 6000??$
Damping	$\sigma_r$ (s <sup>-1</sup> )	5*
Eff. surface area	$S_r$ (m <sup>2</sup> )	$1.46 \cdot 10^{-5}^*$
Width	$w_r$ (m)	0.01*
Equilibrium	$H_0$ (m)	$2.9 \cdot 10^{-4}^*$

Table 1: List of parameter values used for the simulation. Taken from \* [4], \* [3] or \*\* [5] with temperature  $T = 26.85^\circ C$ .

where  $q$  is the pressure of the right side of the tube. Though the paper shows changes in the wavespeed  $c$  rather than the length  $L$ , the effect of a change in either of these parameters has an identical effect on the system.

As long as the geometry is unchanged for the grid points.

To stick to what is physically logical,  $L$  is changed

One can change the

As the geometry varies it matters a lot where points are added and subtracted.

### 5. IMPLEMENTATION

#### 5.1. Parameters

#### 5.2. Order of Calculation

### 6. CONCLUSION AND FUTURE WORK

Investigate the possibility of adding / removing grid points at points where the cross-sectional area is varying.

### 7. REFERENCES

- [1] H. Levine and J. Schwinger, "On the radiation of sound from an unflanged circular pipe," *Physical Review*, vol. 73, no. 2, pp. 383–406, 1948.
- [2] F. Silva, P. Guillemain, J. Kergomard, B. Mallaroni, and A. Norris, "Approximation formulae for the acoustic radiation impedance of a cylindrical pipe," *Journal of Sound and Vibration*, vol. 322, pp. 255–263, 2009.
- [3] Reginald Langford Harrison-Harsley, *Physical Modelling of Brass Instruments using Finite-Difference Time-Domain Methods*, Ph.D. thesis, University of Edinburgh, 2018.
- [4] Tamara Smyth and Frederick S. Scott, "Trombone synthesis by model and measurement," *EURASIP Journal on Advances in Signal Processing*, 2011.
- [5] A. H. Benade, "On the propagation of sound waves in a cylindrical conduit," *Journal of the Acoustical Society of America*, vol. 44, no. 2, pp. 616–623, 1968.

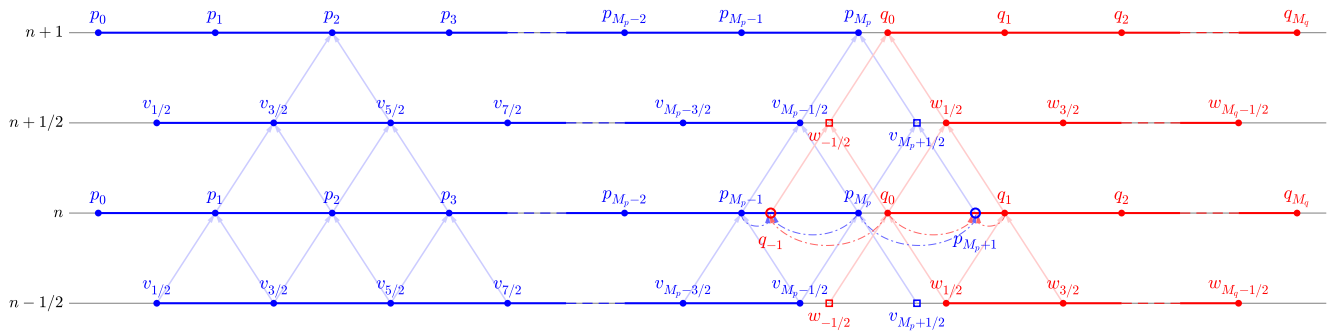


Figure 3: Schematic showing data flow of how different grid points at time index  $n + 1$  are calculated. To prevent cluttering, arrows going straight up (indicating that the state of a grid point at time step  $n$  is needed to calculate the state of that grid point at  $n + 1$ ) are suppressed. As an example of the usual case, the points required to calculate  $p_2^{n+1}$  are shown. Furthermore, the points needed to calculate  $p_{M_p}^{n+1}$  and  $q_0^{n+1}$  are shown. The most important difference with the usual case is that the virtual grid points  $q_{-1}^n$  and  $p_{M_p+1}^n$  are calculated from known values of  $p^n$  and  $q^n$  as opposed to values of  $v^{n-1/2}$  and  $w^{n-1/2}$ .

- [6] S. K. Mitra and J. F. Kaiser, Eds., *Handbook for Digital Signal Processing*, J. Wiley & Sons, New York, NY, USA, 1993.
- [7] Simon Haykin, *Adaptive Filter Theory*, Prentice Hall, Englewood Cliffs, NJ, USA, second edition, 1991.
- [8] X. Serra, *Musical Signal Processing*, chapter Musical Sound Modeling with Sinusoids plus Noise, pp. 91–122, G. D. Poli, A. Piccilli, S. T. Pope, and C. Roads Eds. Swets & Zeitlinger, Lisse, Switzerland, 1996.
- [9] James A. Moorer, “Audio in the new millennium,” *J. Audio Eng. Soc.*, vol. 48, no. 5, pp. 490–498, May 2000.
- [10] A. Nackaerts, B. De Moor, and R. Lauwereins, “Parameter estimation for dual-polarization plucked string models,” in *Proc. Intl. Computer Music Conf.*, Havana, Cuba, Sept. 17–23, 2001, pp. 203–206.
- [11] D. Arfib, “Different ways to write digital audio effects programs,” in *Proc. Digital Audio Effects (DAFx-98)*, Barcelona, Spain, Nov. 19–21, 1998, pp. 188–91.
- [12] A. Askenfelt, “Automatic notation of played music (status report),” Tech. Rep., STL-QPSR, Vol. 1, pp. 1–11, 1976.
- [13] E. B. Egozy, “Deriving musical control features from a real-time timbre analysis of the clarinet,” M.S. thesis, Massachusetts Institute of Technology, 1995.
- [14] P. Dutilleul, *Vers la machine à sculpter le son, modification en temps-réel des caractéristiques fréquentielles et temporelles des sons*, Ph.D. thesis, University of Aix-Marseille II, 1991.
- [15] K. Fitz and L. Haken, “Current Research in Real-time Sound Morphing,” Available at <http://www.cerlsoundgroup.org/RealTimeMorph/>, accessed March 08, 2006.